

Influence of La_2O_3 loading on SnO_2 based sensors

C. V. GOPAL REDDY, S. V. MANORAMA*, V. J. RAO

Materials Science Group, Inorganic and Physical Chemistry Division, Indian Institute of Chemical Technology, Hyderabad-500 007, India
E-mail: manorama@iict.ap.nic.in

Influence of La_2O_3 loading on the structural and gas sensing properties of SnO_2 have been studied. The effect of different weight percentages of La_2O_3 (1–10 wt.%) in SnO_2 , and the effect of calcination temperature on the sensitivity to various reducing gases like LPG, H_2 and CH_4 has been studied. The structural characteristics have been investigated by X-ray diffraction, and the corresponding crystallite size estimated. In addition to the systematic variation in the crystallite size as a function of the sintering temperature, the role of La_2O_3 as an effective grain growth inhibitor has been confirmed. Increasing the percentage of La_2O_3 above 2 wt.% has no added advantage in terms of improving the gas sensing characteristics and also in stabilizing the SnO_2 surface. Once the $\text{La}_2\text{Sn}_2\text{O}_7$ formation temperature is reached, the sensitivity of the sensor decreases marginally. At this temperature the crystallite size also increases very abruptly. All these have been correlated with the formation of the $\text{La}_2\text{Sn}_2\text{O}_7$, a new phase with standard pyrochlore structure.

© 2000 Kluwer Academic Publishers

1. Introduction

Semiconductor gas sensors based on tin oxide detect reducing gases from a change in conductivity. It is generally accepted that the chemisorption of oxygen on the surface of SnO_2 particles creates a high electric resistance layer up to the depth of Debye length (L). Consumption of chemisorbed oxygen by reducing gases results in an increase in conductivity. The Hall effect measurement by Ogawa *et al.* [1] has revealed that ' L ' for a porous thin film of SnO_2 is as small as about 3 nm at 300 °C. On the other hand, the crystallite size of SnO_2 particles (D) in conventional sensor elements is usually in the order of a few tens nanometer. [1]

Yamazoe *et al.* have established that the microstructure of SnO_2 sensor elements can be controlled over a wide range by the addition of small amounts of foreign oxides. The value of D can be controlled by the choice of additive and/or calcination temperature. They observed that the gas sensitivity to hydrogen, carbon monoxide or butane increased as the crystallite size decreased in the range below 10 nm [2]. The stabilisation effect of lanthana in titanium oxide support has been demonstrated by LeDue *et al.* The thermal stability was assessed using BET surface area and XRD [3].

The incorporation of the additives homogeneously can be achieved by adopting either the technique of co-precipitation or sol-gel synthesis. In both these techniques the starting materials are mixed in solution which is an advantage to obtain compositional homogeneity of the powder and as a result, the microstructural homogeneity of the fired product. Co-precipitation is also more efficient than the conventional solid state reaction of ceramic powders [4, 5]. The procedure is

particularly effective for preparing fine powders of the proper composition for multi-component system, because the complicated repetitive steps of the solid state reaction are replaced by single step or low temperature processing methods. Lanthanum oxide incorporated SnO_2 has been shown to be a promising material for sensing CO_2 in dry air with very high and linear variation of sensitivity with gas concentration and also quick response [6].

In this communication we report the studies on lanthanum oxide which was incorporated into SnO_2 to act as a grain growth inhibitor. The effect of variation of the percentage composition of La_2O_3 in SnO_2 on the gas sensing characteristics has been studied. This has been correlated with the crystallite size and also the formation of lanthanum stannate.

2. Experimental details

A powder composed of semiconductor SnO_2 incorporated with varying amounts of La_2O_3 (1–10 wt.%), were prepared by the sol-gel [7] method. To obtain this, corresponding amount of SnCl_4 (Spectrochem) and $\text{La}(\text{NO}_3)_3 \cdot 5\text{H}_2\text{O}$ (Aldrich) were dissolved separately in ethanol (E.Merck Chemical Co.) and D.I water (18 M Ω). The aqueous and alcoholic solutions were then mixed to form an aqua-alcoholic mixture of $\text{La}(\text{NO}_3)_3 \cdot 5\text{H}_2\text{O}$ and SnCl_4 . This solution was kept stirring for 24 h at 50 °C. After a period of aging at a constant temperature, the solution becomes increasingly cloudy and a gelatinous suspension is formed. The stirring was then stopped and the precipitate was allowed to settle. The suspension contracts and settles to

* Author to whom all correspondence should be addressed.

the bottom of the container. The top portion of the solution is then siphoned out and discarded, with minimum disturbance to the gelatinous sediment underneath and replenished with fresh water alcohol mixture. This replenishment procedure is repeated several times to get rid of the chloride content. The sediment was filtered and washed thoroughly with DI water. The absence of chloride ion was confirmed by testing the filtrate with silver nitrate solution. The precipitate was first dried on a water bath, and then in an oven at 120 °C for 12 h. The dried mass was calcined at different temperatures from 500 to 1000 °C for 2 h, to decompose the hydroxides to the respective oxides and thereafter to observe the steady growth of crystallites.

For phase identification and to evaluate the crystallite size, an X ray diffractometer (Siemens D/5000) was used with filtered Cu-K α radiation. X-ray diffraction analysis revealed the presence of SnO $_2$ with the Cassiterite structure. The effect of the La $_2$ O $_3$ on the base material was studied by comparing the XRD spectra of pure SnO $_2$ with that of SnO $_2$: La $_2$ O $_3$ (2 wt.%) and SnO $_2$: La $_2$ O $_3$ (10 wt.%). These two compositions were chosen for our studies to bring out the salient features of our studies. 1 wt.% La $_2$ O $_3$ in SnO $_2$ does not show any significant change neither in the grain size controlling nor in the sensing characteristics. This is obviously after knowing the properties of La $_2$ O $_3$ which is known to stabilize the surface and not allow further grain growth i.e. it acts as a grain growth inhibitor. The Scherrer formula [8] was used to estimate the crystallite size. The composition of the materials was confirmed by energy dispersive analysis of X-rays (EDAX). This was carried out on an EDAX system (Oxford, Link ISIS-300) attached to a scanning electron microscope (SEM-Hitachi S-520).

To fabricate a sensor element, the SnO $_2$: La $_2$ O $_3$ was mixed with an aqueous solution of 2% poly-vinyl alcohol, PVA (binder) and the resulting paste was applied onto alumina tube substrates provided with two platinum wires as electrodes. The element was then sintered at 600 °C for 2 h in air, to impart it ceramic properties. The details of the procedure for preparation of sensor elements have been described earlier [9, 10]. Here the schematic of the experimental setup used for the testing of elements is also shown. The sensitivity, S is defined as the ratio of change in resistance of the sensor in presence of gas, ΔR to the value of the resistance in air, R_a .

$$S = \Delta R/R_a = |R_a - R_g|/R_a \quad (1)$$

3. Results and discussions

Fig. 1 shows the XRD pattern of 2 wt.% La $_2$ O $_3$ incorporated SnO $_2$ calcined at different temperatures from 500–1000 °C. These spectra have been drawn as a function of increasing calcination temperature, Fig. 1a–f. To begin with the mixture is amorphous. It starts to becoming crystalline with the appearance of the characteristic SnO $_2$ peaks at $d = 3.35$, $d = 2.64$, $d = 2.37$ and $d = 1.765$. These peaks continuously get sharper with increasing calcination temperature. As observed we do not expect any peaks due to La $_2$ O $_3$. It is seen that at about 500 °C the peaks just start to appear and as

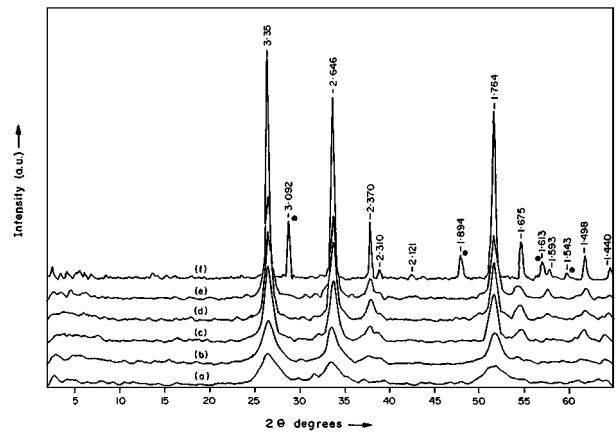


Figure 1 (a–f) The XRD pattern of 2 wt.% La $_2$ O $_3$ incorporated SnO $_2$ calcined at different temperatures from 500–1000 °C.

the temperature is increased the peaks become sharper. This is indicative of the increase in crystalline size. At about 1000 °C the peaks due to La $_2$ Sn $_2$ O $_7$ appear. These have been indicated with dark circles on the spectrum. These positions agree with standard data (JCPDS Card No.: 13-82) [11]. Using the FWHM values of the peaks the crystallite sizes at the different calcination temperature are estimated and tabulated in Table I.

Fig. 2 shows the XRD pattern of 10 wt.% La $_2$ O $_3$ incorporated SnO $_2$, calcined at different temperatures from 500–1000 °C a–g. These spectra have been pure SnO $_2$ calcined at 900 °C included as a reference. As in the previous it is seen that at about 500 °C the SnO $_2$

TABLE I SnO $_2$ crystallite sizes in (a) pure SnO $_2$ (b) SnO $_2$: La $_2$ O $_3$ (2 wt.%) (c) SnO $_2$: La $_2$ O $_3$ (10 wt.%), as a function of calcination temperature

Calcination temperature/ °C	Crystallite size in Å		
	SnO $_2$	SnO $_2$: La $_2$ O $_3$ (2 wt.%)	SnO $_2$: La $_2$ O $_3$ (10 wt.%)
500	113	41.6	28.2
600	181	54.6	36.2
700	227	85.8	80.5
800	240	96.0	94.5
900	259	98.9	100.5
1000	302.5	241.2	302.1

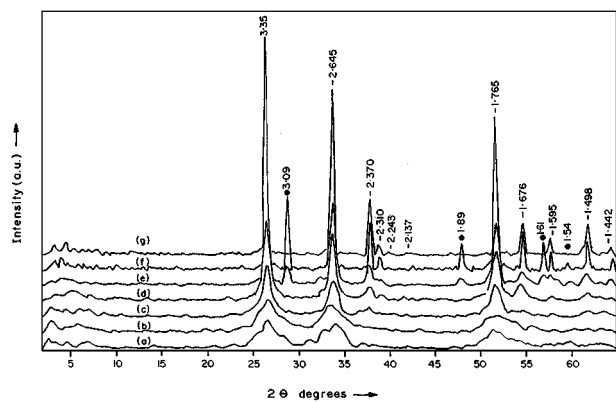


Figure 2 (a–f) The XRD pattern La $_2$ O $_3$ of 10 wt.% La $_2$ O $_3$ incorporated SnO $_2$ at different temperatures from 500–1000 °C. (g) XRD of pure SnO $_2$ calcined at 900 °C.

peaks just appear and become sharper as the calcination temperature is increased indicative of an increase of crystallite size. It is interesting to note that even in this case i.e. with 10 wt.% La_2O_3 in SnO_2 no peaks due to La_2O_3 are observed. The possible reasons for this could be that either La_2O_3 is amorphous or in a highly dispersed state in the matrix. The $\text{La}_2\text{Sn}_2\text{O}_7$ peaks which agree with reported data start appearing at a slightly lower temperature around 900°C itself as opposed to the spectra of SnO_2 : La_2O_3 (2 wt.%). The reason for this difference could be that even though lanthanum stannate formation must have been initiated at 900°C but the composition must be below the detection limit of XRD. But at 1000°C complete conversion would have taken place and hence is observed. The expected composition of $\text{La}_2\text{Sn}_2\text{O}_7$ which could be formed from 2 wt.% La_2O_3 is 6 wt.%.

Table I gives the values of the SnO_2 crystallites in (a) pure SnO_2 (b) SnO_2 : La_2O_3 (2 wt.%) (c) SnO_2 :

La_2O_3 (10 wt.%). It is seen that the effect of grain growth inhibition is valid only as long as the $\text{La}_2\text{Sn}_2\text{O}_7$ formation does not take place. At lower concentrations of La_2O_3 there is better dispersion and the role of preventing grain growth as a function of calcination temperature, is more effective. As the composition of the additive is increased and so also the calcination temperature, $\text{La}_2\text{Sn}_2\text{O}_7$ formation takes place more easily, this probably coats the individual SnO_2 particles. This results in an increase in the electrical resistance of the sensor in air, R_a . But this does not directly show itself in any improvement in the sensitivity.

The scanning electron micrographs, SEM also show the same trend as what is observed in the XRD spectra. Fig. 3a is the SEM micrograph of pure SnO_2 calcined at 900°C as a reference. Fig. 3b and c are those of SnO_2 : La_2O_3 (2 wt.%) calcined at 600°C and 900°C respectively and (d) and (e) are those for SnO_2 : La_2O_3 (10 wt.%) calcined at 600°C and 900°C respectively.

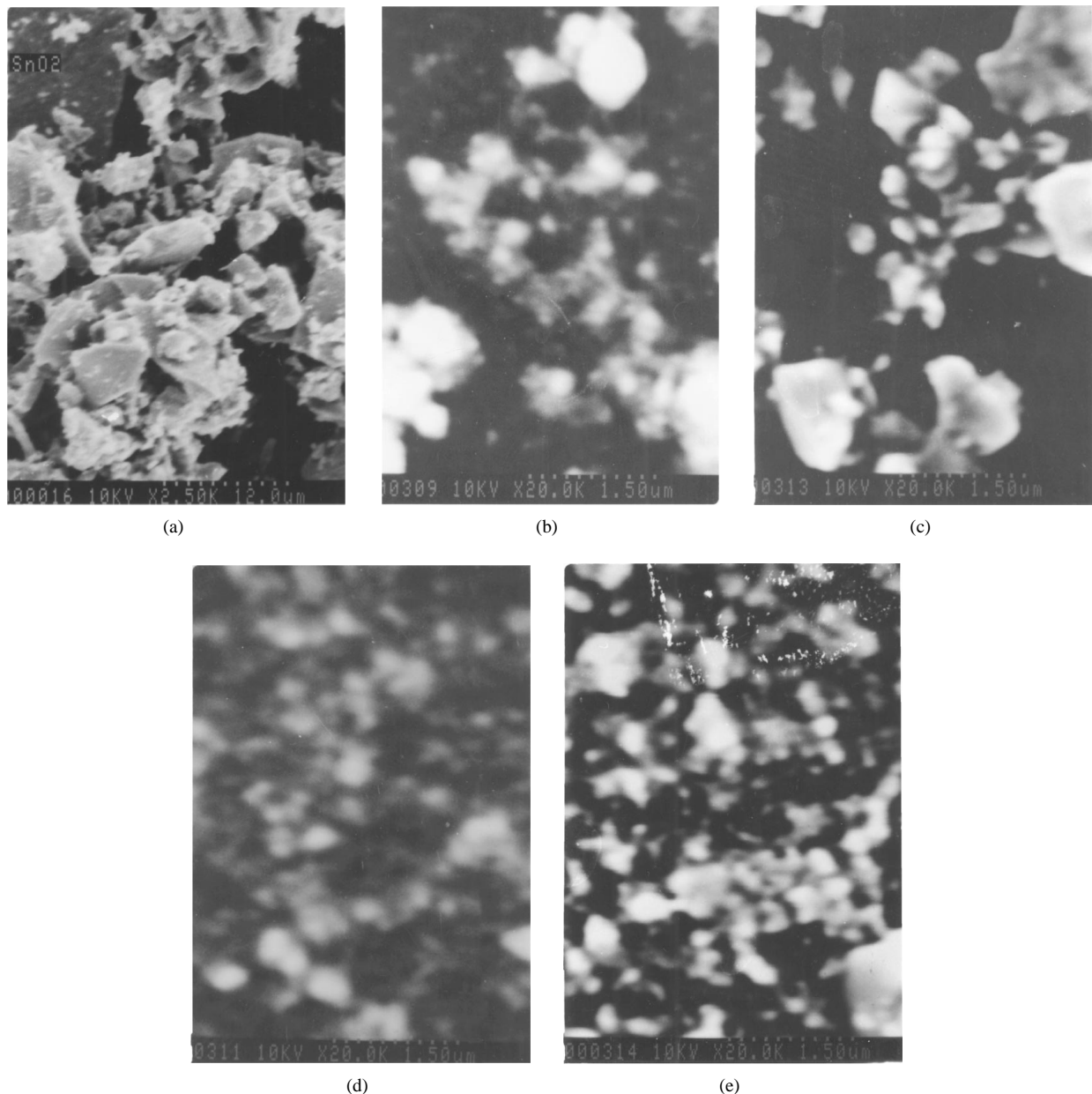


Figure 3 SEM micrographs of (a) Pure SnO_2 calcined at 900°C , (b) SnO_2 : 2 wt.% La_2O_3 calcined at 600°C , (c) SnO_2 : 2 wt.% La_2O_3 calcined at 900°C , (d) SnO_2 : 10 wt.% La_2O_3 calcined at 600°C (e) SnO_2 : 10 wt.% La_2O_3 calcined at 900°C .

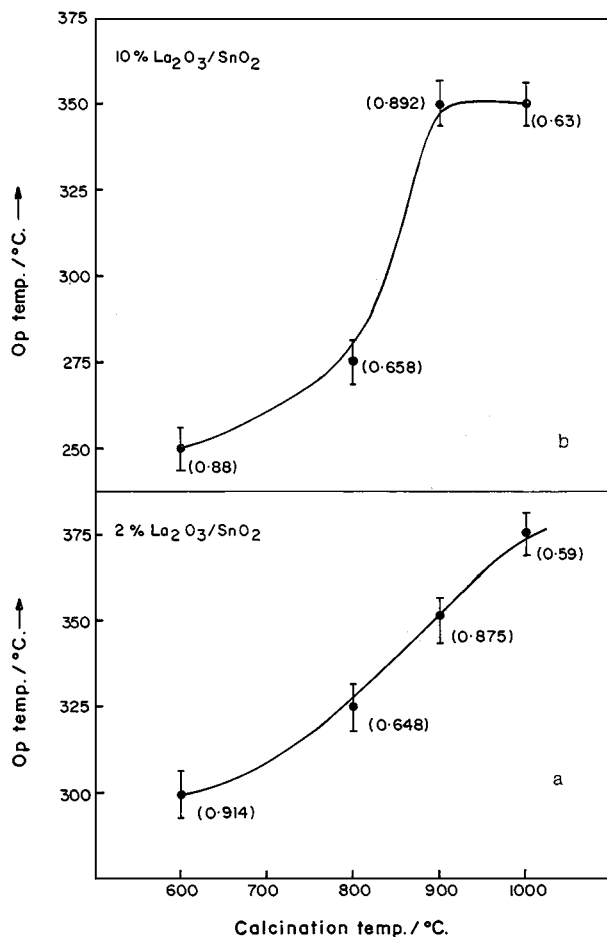


Figure 4 Gas sensing characteristics, variation of operating temperature as a function of calcination temperature for maximum sensitivity (a) SnO₂: 2 wt.% La₂O₃, (b) SnO₂: 10 wt.% La₂O₃.

We observe a clear increase in the crystallite size as the calcination temperature is increased from 600 to 900 °C. This change is more pronounced in the 2 wt.% La₂O₃ sample. This could be attributed to a better dispersion of the 2 wt.% La₂O₃ as compared to the 10 wt.% La₂O₃ and also in the latter there is a higher probability for segregation to take place. The SEM micrographs show the crystallites in the 10 wt.% La₂O₃/SnO₂ as smaller aggregates well separated with an ultimate size around 0.05 or 0.1 μm. The difference in the 600 °C and 900 °C annealed sample is the coming together of the aggregates to form larger crystallites. The crystallites in the 2 wt.% La₂O₃/SnO₂ system are larger with an ultimate crystallite size not less than 0.2 or 0.3 μm.

To have an idea of the distribution of the size of the crystallites one representative sample has been analyzed on a Malvern instruments EASY particle analyzer. It is seen that 2 wt.% La₂O₃/SnO₂ and calcined at 600 °C the particles are distributed in a range of sizes between 3.0 to 28 μm with a maximum around 8–10 μm.

We have studied the gas sensing characteristics of La₂O₃: SnO₂ calcined at different temperatures to different gases like H₂, LPG and CH₄. The sensitivity of the sensors to hydrogen is extraordinarily high so we were not able to establish any trend in the sensitivities as a function of the different parameters like % of La₂O₃ and the calcination temperature. Converse is the

case for CH₄, which does not show any reasonable sensitivity even upto 250 °C. So in this paper we report our studies only on LPG to elaborate our findings on the effect of the different parameters on the gas sensing characteristics.

Fig. 4 shows the gas sensing characteristics of SnO₂ with (a) 2 wt.% La₂O₃ and (b) 10 wt.% La₂O₃ response to LPG. The results have been presented in such a way that the effect of maximum sensitivity on two parameters namely the operating temperature and the calcination temperature can be directly observed. The figures show the operating temperature where you observe the maximum sensitivity as a function of the calcination temperature for two compositions. The values in the parenthesis indicate the maximum sensitivities observed.

From these results there are some very striking observations. The percentage of La₂O₃ in SnO₂ has the following effects:

- (1) Increase in La₂O₃ seems to shift the operating temperature for maximum sensitivity to the lower side.
- (2) Another observation is the resistance of the sensor in air of 2 wt.% La₂O₃/SnO₂ is less than that of 10 wt.% La₂O₃/SnO₂. This could be attributed to higher content of La₂Sn₂O₇, a highly insulating material which coats the individual SnO₂ crystallites.

4. Conclusions

Our studies bring out a definite trend in the dependence of the crystallite size of SnO₂ and indirectly the sensitivity to reducing gases. These also establish a relation between the structure i.e. the size of the crystallite and property i.e. the gas sensing characteristics. The effect of La₂O₃ on SnO₂ as an effective grain growth inhibitor has been demonstrated. La₂Sn₂O₇ formation has been shown to inhibit the grain size control and also to reduce the sensitivity. These results are only indicative and to establish a definite mechanism as to the role of La₂O₃ in stabilizing the SnO₂ surface further experimentation is underway.

Acknowledgements

The authors gratefully acknowledge the financial support of DST, New Delhi. One of the authors CVGR thanks CSIR, New Delhi for the Senior Research Fellowship.

References

1. H. OGAWA, M. NISHIKAWA and A. ABE, *J. Appl. Phys.* **53** (1982) 4448.
2. C. XU, J. TAMAKI, N. MIURA and N. YAMAZOE, *Chem. Letts.* (1990) 441.
3. CHARLES A. LEDUC, JEFFREY M. CAMPBELL and JOSEPH A. ROSSIN, *Ind. Eng. Chem. Res.* **35** (1996) 2473.
4. D. W. JOHNSON, JR. and P. K. GALLAGHER, in "Ceramic Processing Before Firing," edited by G. Y. Onoda, Jr., and L. L. Hench (Wiley, New York, 1978) p. 125.
5. E. MATIJEVIC, in "Science of Ceramic Chemical Processing," edited by L. L. Hench and D. R. Ulich. (Wiley, New York, 1986) p. 463.

6. T. YOSHIOKA, N. MIZUNO and M. IWAMOTO, *Chem. Letts.* (1992) 1249.
7. NAE-LIH WU, LIH-FU WU, YA-CHIN YANG and SHU-JIUAN HUANG, *J. Materials Research* **11** (1996) 4813.
8. H. P. KLUG and L. E. ALEXANDER, "X-ray Diffraction Procedures for Polycrystalline and Amorphous Materials" (John Wiley, New York; Chapman & Hall, London, 1974), p. 491.
9. S. MANORAMA, G. SARALA DEVI and V. J. RAO, *Appl. Phys. Letts.* **64** (1994) 3163.
10. L. SATYANARAYANA, C. V. GOPAL REDDY, S. V. MANORAMA and V. J. RAO, *Sensors and Actuators B* **46** (1998) 1.
11. CHARLES G. WHINFREY, DONALD. W. ECKART and ARTHUR TAUBER, *J. Amer. Chem. Soc.* **82** (1960) 2695.

*Received 25 February
and accepted 15 December 1999*